


The magnetization profile induced by the double magnetic proximity effect in an Fe/Fe_{0.30}V_{0.70} superlattice

Cite as: Appl. Phys. Lett. **115**, 012406 (2019); <https://doi.org/10.1063/1.5102121>

Submitted: 24 April 2019 . Accepted: 21 June 2019 . Published Online: 03 July 2019

H. Palonen , B. O. Mukhamedov, A. V. Ponomareva, G. K. Pálsson, I. A. Abrikosov, and B. Hjörvarsson



View Online



Export Citation



CrossMark

ARTICLES YOU MAY BE INTERESTED IN

[Structural, magnetic, and electrical properties of collinear antiferromagnetic heteroepitaxy cubic Mn₃Ga thin films](#)

Applied Physics Letters **115**, 012402 (2019); <https://doi.org/10.1063/1.5088790>

[Spin-current diode with a monoaxial chiral magnet](#)

Applied Physics Letters **115**, 012401 (2019); <https://doi.org/10.1063/1.5097866>

[Bose-Einstein condensation of mexons in hematite at +210 °C](#)

Applied Physics Letters **115**, 012407 (2019); <https://doi.org/10.1063/1.5096409>



The magnetization profile induced by the double magnetic proximity effect in an Fe/Fe_{0.30}V_{0.70} superlattice

Cite as: Appl. Phys. Lett. **115**, 012406 (2019); doi: [10.1063/1.5102121](https://doi.org/10.1063/1.5102121)

Submitted: 24 April 2019 · Accepted: 21 June 2019 ·

Published Online: 3 July 2019



View Online



Export Citation



CrossMark

H. Palonen,^{1,a)} B. O. Mukhamedov,² A. V. Ponomareva,² G. K. Pálsson,¹ I. A. Abrikosov,³ and B. Hjörvarsson¹

AFFILIATIONS

¹Materials Physics, Department of Physics and Astronomy, Uppsala University, Box 530, SE-75121 Uppsala, Sweden

²Materials Modeling and Development Laboratory, National University of Science and Technology (MISIS), 119049 Moscow, Russian Federation

³Department of Physics, Chemistry and Biology, Linköping University, SE-58183 Linköping, Sweden

^{a)}Author to whom correspondence should be addressed: heikki.palonen@utu.fi

ABSTRACT

The double magnetic proximity effect (MPE) in an Fe/Fe_{0.30}V_{0.70} superlattice is studied by a direct measurement of the magnetization profile using polarized neutron reflectivity. The experimental magnetization profile is shown to qualitatively agree with a profile calculated using density functional theory. The profile is divided into a short range interfacial part and a long range tail. The interfacial part is explained by charge transfer and induced magnetization, while the tail is attributed to the inhomogeneous nature of the FeV alloy. The long range tail in the magnetization persists up to 170% above the intrinsic ordering temperature of the FeV alloy. The observed effects can be used to design systems with a direct exchange coupling between layers over long distances through a network of connected atoms. When combined with the recent advances in tuning and switching, the MPE with electric fields and currents, the results can be applied in spintronic devices.

Published under license by AIP Publishing. <https://doi.org/10.1063/1.5102121>

The magnetic equivalent of the superconducting proximity effect is the magnetic proximity effect (MPE), which manifests as a region of enhanced magnetization at an interface between two ferromagnets (FMs) or between a FM and a nonmagnetic (NM) material. There are at least four different types of MPE that can occur: (i) In FM/NM systems, the hybridization of electron orbitals leads to a charge transfer across the interface. If the charge transfer favors one spin state more than the other, the nonmagnetic material will become locally spin polarized with an extension of few atomic layers. An example of charge transfer induced MPE is the Fe/V system where the first few V layers have a magnetic moment that is antiferromagnetically aligned with respect to the moment of the Fe layer.¹ (ii) There is an additional induced MPE at increased temperatures in a FM/FM system, which can be rationalized by the high susceptibility of the weaker FM layer in the paramagnetic (PM) state above its ordering temperature.² (iii) If the NM layer of the FM/NM system is close to fulfilling the Stoner criterion, a strong MPE can be expected.^{3–5} However, it is not always observed in such systems.^{6,7} (iv) Magnetic heterostructures composed of alloys have been shown to exhibit large magnetic proximity effects,

irrespective of the crystalline ordering, for example, in amorphous CoAlZr alloys or in the crystalline FeV alloys of the present work.⁸

In this paper, cases (i)–(ii) are referred to as the interfacial MPE and case (iv) as chemical disorder MPE. A random alloy is not uniform in the atomic picture. Instead, there are regions with higher and lower chemical compositions than the average. The regions make the alloy intrinsically inhomogeneous which is here referred to as chemical disorder.

An increased understanding of the origin of different types of MPE is needed to have full control of the interface phenomena in magnetic heterostructures. For example, MPE is often accompanied by exchange bias, and it is involved in the generation of spin currents in nonmagnetic metals and can be used to push up the ordering temperature of dilute magnetic semiconductors and topological insulators.^{3,9–11} Furthermore, the MPE can be used to induce a moment above the Néel temperature in an antiferromagnetic system.¹² The relevance of MPE for applications is further emphasized by the recent findings of Yamada *et al.* and Koyama *et al.* who showed that the magnitude of the MPE can be tuned with the electric field and that the

magnetic moment in the MPE can be switched without switching the source.^{13,14}

The double proximity effect is a combination of a finite size effect and an interfacial MPE, resulting in a situation where a component is magnetic only because the other component is exerting MPE on it and vice versa. Previously, we have shown that there are strong double proximity effects in Fe/FeV superlattices where the ordering temperature of the FeV alloy was doubled by the proximity of a single monolayer (ML) of Fe and the Fe layers were enhancing each other's ordering temperature across 30 ML (4.5 nm) of the FeV alloy.² While the long range of the exchange interaction between the Fe monolayers was demonstrated, not much could be concluded about the underlying mechanism using only average saturation magnetizations. Thus, direct measurements of the magnetization profile inside the structure are needed to gain more information on the mechanism.

In this paper, the focus is on the magnetization profile of a single ML of Fe in the Fe_{0.30}V_{0.70} alloy which is schematically shown in Fig. 1. The profile is studied in a superlattice where the thickness of the alloy layer separating the Fe layers is 30 ML. The samples were grown by magnetron sputtering, and the FeV alloy was done by cosputtering. The FeV alloy composition (30 at. % Fe) was determined by measuring the ordering temperature (60 K) of the FeV reference alloy grown separately with the same growth parameters and comparing with the work of Mustafa and Read.¹⁵ More details of the sample preparation are available in the [supplementary material](#).

The magnetic moment of the bilayer can be divided into three parts: the magnetization of the source, a long tail of the magnetization extending far into the alloy together with the spontaneous magnetization of the alloy, and the interfacial MPE region which decreases rapidly when moving away from the interface. The three regions are highlighted with different colors in Fig. 1. The interfacial MPE region arises from the charge transfer and high susceptibility of the alloy. If the tails of two nearest source layers overlap, the source layers will interact, which leads to an increase in the ordering temperature.

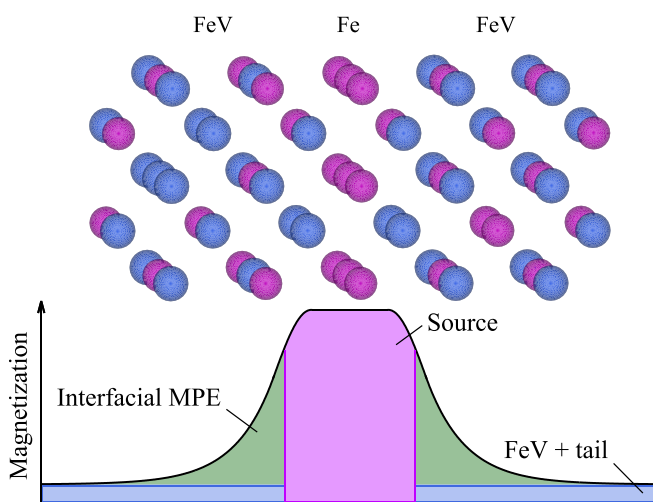


FIG. 1. A schematic of the sample structure (top) showing 1 ML of Fe inserted inside an FeV alloy. A schematic of the magnetization profile (bottom) of the structure. The profile has been divided into regions (colors) that mark the different parts of the MPE.

The theoretical magnetization profile of the superlattice was calculated in the framework of the density functional theory (DFT) using the exact muffin-tin orbitals (EMTO) method combined with the coherent potential approximation.^{16,17} The EMTO method uses the Green's function technique to solve the multiple scattering problem. The generalized gradient approximation was used to describe the exchange and correlation effects (see the [supplementary material](#) for more details).¹⁸

Experimentally, the magnetization profile in the Fe/FeV superlattice can be measured by polarized neutron reflectivity (PNR) which gives a direct measurement of the spatial shape of the magnetic flux density in the sample. The PNR of the Fe/FeV superlattice was measured at the SuperADAM reflectometer at the Institut Laue Langevin in Grenoble, France.¹⁹ The PNR data were fitted using GenX.²⁰ More details of the PNR experiment and the fitting procedure are available in the [supplementary material](#). Examples of the spin up-up, down-down reflectivities and their difference are shown in Fig. 2(a). The excellent quality of the measurement and the sample is emphasized by the fact that it was possible to measure very high in Q_z , up to 0.55 \AA^{-1} , where the fourth Bragg peak is still visible above the background.

A model that consists of the three parts shown by the colored areas in Fig. 1 was used for fitting the measured PNR data. The magnetization of the source was approximated with a 3-ML-thick constant value. Considering the combination of the atomic steps smearing out, the PNR results, and the double peak structure near the Fe layer (to be discussed below), the approximation should be fairly good. In addition, the approach will be consistent with our previous work where the same approximation was used.² The interfacial MPE profile was modeled with an exponentially decreasing magnetization with the

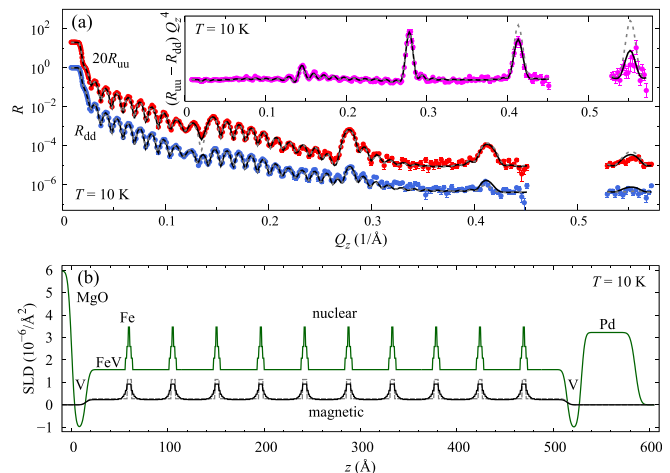


FIG. 2. (a) The PNR of the sample at 10 K shown on a logarithmic scale. The up-up reflectivity (R_{uu}) is shifted from the down-down reflectivity (R_{dd}) for clarity. The solid and dashed lines are the best fits with and without the interfacial MPE in the model, respectively. Inset: The difference of the up-up and down-down reflectivities scaled with Q_z^4 shown on a linear scale. (b) The scattering length density (SLD) corresponding to the best fits with (solid) and without (dashed) the interfacial MPE. The nuclear SLD is determined by the elemental composition profile of the sample and the magnetic SLD by the magnetization profile. The up-up (down-down) reflectivity means that both the incident and reflected neutrons are spin up (down). The SLD corresponding to the up-up (down-down) reflectivity is the sum (difference) of the nuclear and magnetic SLD.

increasing distance from the source. The exponential profile is to be expected if the interfacial MPE is considered to be induced by the magnetization of the neighboring layer.^{1,2} Only three free parameters were used in fitting the magnetization profile of the superlattice: the strength of the source, M_δ , the spatially constant magnetization of the FeV layer, M_{FeV} , and the characteristic length scale of the exponential function, ξ . The magnetization profile in the first half of the FeV layer is

$$M(x) = (M_\delta - M_{\text{FeV}}) \exp\left(-\frac{x}{\xi}\right) + M_{\text{FeV}}, \quad (1)$$

where x is the distance from the Fe layer interface. An example of the magnetization profile is shown in Fig. 2(b) together with the nuclear SLD of the superlattice. In Fig. 2, the solid (dashed) line shows the best fit and the corresponding SLD profile of the superlattice with (without) the interfacial MPE. Comparing the difference between the fits given by the models, it can be seen that the model with the MPE included is more consistent with the data. Also, the first and the second order Bragg peaks are virtually unaffected by the shape of the magnetization profile near the Fe layer interface, which emphasizes the importance of collecting enough Fourier components to be able to measure interfacial MPE.

According to the DFT calculation, the average magnetic moment per atomic site in the superlattice has a maximum at the source, as can be seen in Fig. 3. A double peak structure can be seen in the source when looking at the moments per Fe atom, which arises from the change of Fe coordination of the Fe atoms at the source layer: All the nearest neighbors of an atom inside a (100) body-centered cubic (bcc) monolayer are located in the neighboring layers. As a result, the Fe atoms on the FeV side of the interface always have a higher Fe coordination than the Fe atoms in the single ML of Fe, which leads to the

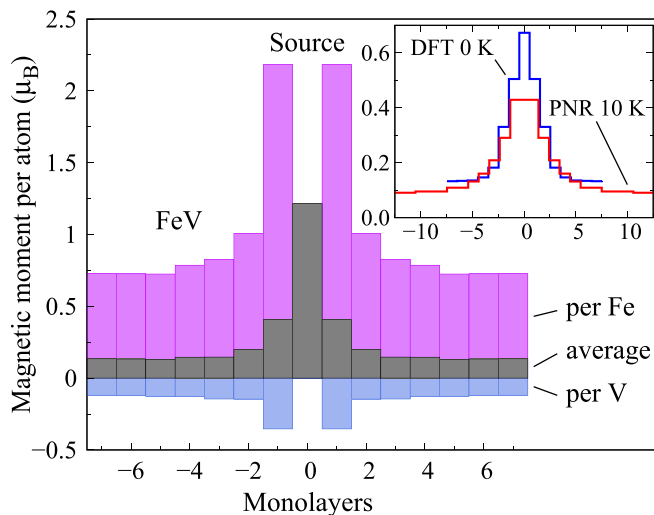


FIG. 3. The magnetic moment per atom and atomic site (average) given by the DFT calculation around the Fe ML, which is the source. The negative values are used to indicate the antiferromagnetic alignment between the Fe and V moments. Inset: The magnetic moment per atomic site around one of the Fe layers according to the PNR fit at 10 K and according to the DFT calculation at 0 K. The latter has been broadened with the nuclear SLD results to make the comparison more realistic. The units in the inset are the same as in the main figure.

double peak structure. The Fe moment reaches the bulk value of $2.2 \mu_B$ on the alloy side of the interface, while in the Fe ML, it is only $1.2 \mu_B$. The effects of the Fe coordination are also clearly visible in the charge transfer results that were calculated from the DFT (see the [supplementary material](#) for the full charge transfer results). The Fe atoms on the FeV side of the interface have almost no charge transfer at all compared to the bulk Fe, which leads to the high Fe moment. The Fe atoms in the Fe monolayer are strongly affected by charge transfer, which is consistent with the weak (compared to bulk Fe) moment of the Fe atoms in the monolayer. For V at the interface, the theory predicts a moment of $0.35 \mu_B$, which is antiferromagnetically aligned with respect to the Fe moments. The enhancement of the antiferromagnetic moment of the V atoms at the interface is also seen in the charge transfer results as a decrease in the V spin up electrons. The antiferromagnetic alignment and a moment of $0.7 \mu_B$ for V at the interface have been previously reported in Fe/V multilayers.¹ By comparison, the DFT calculations underestimate the V moment. The range of the interfacial MPE around the source is about 3 ML according to the calculation.

The PNR fit gives an average moment of $0.43 \mu_B$ and $0.090 \mu_B$ for the source and FeV layer, respectively, per atomic site at 10 K. In our previous work based on vibrating sample magnetometry (VSM), a comparison between the samples resulted in $0.54 \mu_B$ and $0.12 \mu_B$ for the source and FeV layers.² The agreement is quite good considering that VSM gives only indirect information about the magnetization of individual layers, while PNR gives a direct measurement, and that in this work, the alloy has 30% Fe instead of 32% in the previous work.

The magnetization profiles given by the PNR fit and by DFT calculations around one of the source layers are shown in the inset of Fig. 3. To make the comparison between the theoretical and experimental curve more realistic, the DFT profile has been broadened by using the PNR fit result for the nuclear SLD. Since the total amount of Fe atoms in the grown Fe layer corresponds very accurately to what is needed to form a perfect monolayer, the nuclear SLD can be considered as a measure of how those atoms are distributed. This distribution is caused both by sample and instrumental effects; the measurement gives a one dimensional projection of the sample within the coherence volume. Atomic steps, for example, will smear out the resulting profile. The DFT result agrees qualitatively with the experimental profile, but the absolute values are slightly overestimated, which could be due to the underestimated V moments. The range of the interfacial MPE in the experimental result is not very long, only about 3 ML. Thus, the large MPE observed previously in the Fe/FeV has to come from the enhancement of the spatially constant FeV layer moment instead of the interface.²

As mentioned above, the magnetization profile is divided into parts (see Fig. 1) which allows for further analysis by separately looking into the temperature dependencies of the regions. As is shown in Fig. 4, the Fe layer shows higher and the FeV layer smaller moments at all temperatures compared to the average moment. The moment of the FeV layer vanishes at the same temperature as the average moment, showing that the system becomes fully ferromagnetic at a single ordering temperature. The moment in the interfacial MPE region does not decrease monotonically with increasing temperature because it has a large contribution coming from the magnetic susceptibility of the intrinsically paramagnetic alloy in the temperature region above the intrinsic ordering temperature of the FeV alloy.

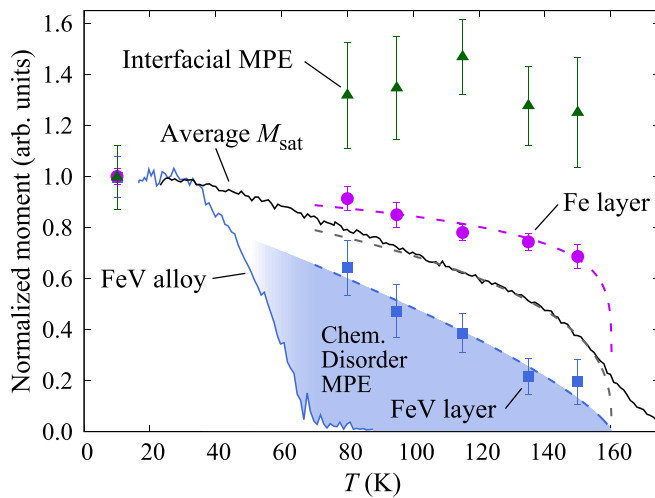


FIG. 4. The temperature dependence of the magnetic moments (points) in the different parts of the magnetization profile as illustrated in Fig. 1. The solid lines are the saturation magnetizations from the MOKE measurements of the superlattice sample and the reference FeV alloy with the same composition as was used in the FeV layer of the superlattice. The dashed lines are fits of Eq. (2). The enhancement of the magnetic moment of the FeV alloy is marked with the colored area.

The magnetization near the ordering temperature scales as

$$M \propto (1 - t)^\beta, \quad (2)$$

where t is the reduced temperature and β is an effective exponent. In this context, β is not considered as a critical exponent since the system is not homogeneous. The moment of the source layer remains high even very close to the ordering temperature. The same behavior was also observed in our previous work and is consistent with a two dimensional (2D) Ising system ($\beta = 0.125$) which is shown as the dashed line in Fig. 4. The fact that the source layer is very thin and anisotropic is consistent with the 2D Ising behavior.² The best fit gives effective exponents of 0.74 and 0.34 for the FeV layer and the average magnetization measured by the magneto-optical Kerr effect (MOKE), respectively. The latter two effective exponents should not be used to draw conclusions about the dimensionality because of the inhomogeneous nature of the system. The effective exponent of the FeV layer is high because of the temperature dependence of its magnetic susceptibility which is similar to what has been observed in Fe/Pd.⁴

The nonvanishing and spatially constant value of the magnetization in FeV between the source layers above the intrinsic ordering temperature of the alloy can be rationalized as a result of a slowly decreasing, almost linear, tail. Consider two tails that originate from the nearest Fe layers with slopes that are similar in magnitude but opposite in sign. When they are added up, the result is an approximately constant value. One possible origin for the long range tail is the chemical disorder of the FeV alloy: The randomness of the alloy is not homogeneous at the atomic scale, which results in chains of connected Fe atoms where the other end of the chain is polarized and fixed by the continuous Fe layer. The chemical disorder is a universal property of random alloys and is likely to be the reason for the very long range MPE observed in $\text{Co}_{60}\text{Al}_{28}\text{Zr}_{12}$ as well.⁸ Choi *et al.* have studied MPE in a Gd/Fe system, which is free of chemical disorder.²¹ The MPE that

they observed is similar to the interfacial part of the MPE in our system, but they observed no long range tail in the Gd layer, which is consistent with our interpretation of the chemical disorder as the origin of the tail. The tail is not observed in the DFT calculations because the local environment effects in a system with the chemical disorder would need to be included in the model of the alloy instead of working with the global average composition and because the DFT calculations are done at 0 K, where the FeV alloy is ferromagnetic in any case.

A comparison of the FeV magnetization to the reference alloy shows that the MPE enhances strongly the ordering temperature of FeV, from 60 K to 160 K which is a 170% increase. The enhancement is marked with the colored area in Fig. 4. The fact that the tail of the magnetization profile is constant across 30 ML and that the constant part persists up to the ordering temperature emphasizes the long range of the MPE at all temperatures.

In conclusion, the magnetization profile of the MPE at an FM/FM and FM/PM interface, where the PM system is above its intrinsic ordering temperature and has chemical disorder, can be rationalized to consist of an interfacial part and a slowly decreasing tail. The tail extends far from the interface, while the interfacial part that originates from induced magnetization and charge transfer effects has a short range. Changes in the Fe coordination are the origin of the charge transfer effects. The strong induction is explained by the high magnetic susceptibility of the FeV alloy above the intrinsic ordering temperature of the alloy. The tail of the MPE is caused by the inhomogeneous nature of the FeV alloy, resulting in an extended network of connected magnetic atoms. The tail has a long range and persists high, up to 170%, above the intrinsic ordering temperature of the alloy. The observed MPE enables additional tunability in the design of magnetic materials, allowing for a direct exchange coupling over long distances through a network of connected atoms. Furthermore, the results are applicable in spintronics when they are combined with the recent advances in tuning and switching the MPE with electric fields and currents.

See the [supplementary material](#) for the complete description of the structure calculations, experimental methods, PNR fits, and charge transfer results.

Financial support from the Swedish Research Council is gratefully acknowledged. The theoretical calculations were supported by the Ministry of Science and High Education of the Russian Federation in the framework of Increase Competitiveness Program of NUST (MISIS) (No. K2-2019-001) implemented by a governmental decree (16th March 2013, No. 211). Financial support from the Swedish Government Strategic Research Areas in Materials Science on Functional Materials at Linköping University (Faculty Grant SFO-Mat-LiU No. 2009-00971) and the Swedish e-Science Centre is gratefully acknowledged.

REFERENCES

- ¹M. A. Tomaz, W. J. Antel, Jr., W. L. O'Brien, and G. R. Harp, "Induced V moments in Fe/V(100), (211), and (110) superlattices studied using x-ray magnetic circular dichroism," *J. Phys.: Condens. Matter* **9**, L179–L184 (1997).
- ²H. Palonen, F. Magnus, and B. Hjörvarsson, "Double magnetic proximity in Fe/Fe_{0.32}V_{0.68} superlattices," *Phys. Rev. B* **98**, 144419 (2018).
- ³S. Y. Huang, X. Fan, D. Qu, Y. P. Chen, W. G. Wang, J. Wu, T. Y. Chen, J. Q. Xiao, and C. L. Chien, "Transport magnetic proximity effects in platinum," *Phys. Rev. Lett.* **109**, 107204 (2012).

- ⁴T. P. A. Hase, M. S. Brewer, U. B. Arnalds, M. Ahlberg, V. Kapaklis, M. Björck, L. Bouchenoire, P. Thompson, D. Haskel, Y. Choi, J. Lang, C. Sánchez-Hanke, and B. Hjörvarsson, "Proximity effects on dimensionality and magnetic ordering in Pd/Fe/Pd trilayers," *Phys. Rev. B* **90**, 104403 (2014).
- ⁵S. Cao, M. Street, J. Wang, J. Wang, X. Zhang, C. Binek, and P. A. Dowben, "Magnetization at the interface of Cr₂O₃ and paramagnets with large stoner susceptibility," *J. Phys.: Condens. Matter* **29**, 10LT01 (2017).
- ⁶S. Geprägs, S. Meyer, S. Altmannshofer, M. Opel, F. Wilhelm, A. Rogalev, R. Gross, and S. T. B. Goennenwein, "Investigation of induced Pt magnetic polarization in Pt/Y₃Fe₅O₁₂ bilayers," *Appl. Phys. Lett.* **101**, 262407 (2012).
- ⁷M. Collet, R. Mattana, J.-B. Moussy, K. Ollefs, S. Collin, C. Deranlot, A. Anane, V. Cros, F. Petroff, F. Wilhelm, and A. Rogalev, "Investigating magnetic proximity effects at ferrite/Pt interfaces," *Appl. Phys. Lett.* **111**, 202401 (2017).
- ⁸F. Magnus, M. E. Brooks-Bartlett, R. Moubah, R. A. Procter, G. Andersson, T. P. A. Hase, S. T. Banks, and B. Hjörvarsson, "Long-range magnetic interactions and proximity effects in an amorphous exchange-spring magnet," *Nat. Commun.* **7**, 11931 (2016).
- ⁹P. K. Manna and S. M. Yusuf, "Two interface effects: Exchange bias and magnetic proximity," *Phys. Rep.* **535**, 61–99 (2014).
- ¹⁰C. Song, M. Sperl, M. Utz, M. Ciorga, G. Woltersdorf, D. Schuh, D. Bougeard, C. H. Back, and D. Weiss, "Proximity induced enhancement of the Curie temperature in hybrid spin injection devices," *Phys. Rev. Lett.* **107**, 056601 (2011).
- ¹¹W. Liu, L. He, Y. Xu, K. Murata, M. C. Onbasli, M. Lang, N. J. Maltby, S. Li, X. Wang, C. A. Ross, P. Bencok, G. van der Laan, R. Zhang, and K. L. Wang, "Enhancing magnetic ordering in Cr-doped Bi₂Se₃ using high-T_C ferrimagnetic insulator," *Nano Lett.* **15**, 764 (2015).
- ¹²S. M. Sutorin, V. V. Fedorov, A. G. Banskchikov, D. A. Baranov, K. V. Koshmak, P. Torelli, J. Fujii, G. Panaccione, K. Amemiya, M. Sakamaki, T. Nakamura, M. Tabuchi, L. Pasquali, and N. S. Sokolov, "Proximity effects and exchange bias in Co/MnF₂(111) heterostructures studied by x-ray magnetic circular dichroism," *J. Phys.: Condens. Matter* **25**, 046002 (2013).
- ¹³K. T. Yamada, M. Suzuki, A.-M. Pradipto, T. Koyama, S. Kim, K.-J. Kim, S. Ono, T. Taniguchi, H. Mizuno, F. Ando, K. Oda, H. Kakizakai, T. Moriyama, K. Nakamura, D. Chiba, and T. Ono, "Microscopic investigation into the electric field effect on proximity-induced magnetism in Pt," *Phys. Rev. Lett.* **120**, 157203 (2018).
- ¹⁴T. Koyama, Y. Guan, Y. Hibino, M. Suzuki, and D. Chiba, "Magnetization switching by spin-orbit torque in Pt with proximity-induced magnetic moment," *J. Appl. Phys.* **121**, 123903 (2017).
- ¹⁵A. Mustafa and D. A. Read, "Magnetic properties of ferromagnetic VFe alloys near the critical concentration for ferromagnetism," *J. Magn. Magn. Mater.* **5**, 349–352 (1977).
- ¹⁶L. Vitos, I. A. Abrikosov, and B. Johansson, "Anisotropic lattice distortions in random alloys from first-principles theory," *Phys. Rev. Lett.* **87**, 156401 (2001).
- ¹⁷L. Vitos, *Computational Quantum Mechanics for Materials Engineers: The EMT Method and Applications* (Springer-Verlag, London, 2007).
- ¹⁸J. P. Perdew, K. Burke, and M. Ernzerhof, "Generalized gradient approximation made simple," *Phys. Rev. Lett.* **77**, 3865 (1996).
- ¹⁹A. Vorobiev, A. Devishvilli, G. Palsson, H. Rundlöf, N. Johansson, A. Olsson, A. Dennison, M. Wollf, B. Giroud, O. Aguetaz, and B. Hjörvarsson, "Recent upgrade of the polarized neutron reflectometer super ADAM," *Neutron News* **26**, 25 (2015).
- ²⁰M. Björck and G. Andersson, "GenX: An extensible X-ray reflectivity refinement program utilizing differential evolution," *J. Appl. Crystallogr.* **40**, 1174 (2007).
- ²¹Y. Choi, D. Haskel, R. E. Camley, D. R. Lee, J. C. Lang, G. Srager, J. S. Jiang, and S. D. Bader, "Temperature evolution of the Gd magnetization profile in strongly coupled Gd/Fe multilayers," *Phys. Rev. B* **70**, 134420 (2004).